Combustion synthesis of Ca-α-SiAlON:Eu^{2+} phosphors with different Ca concentrations and diluent ratios

Genki Saito[a], Yuji Kunisada[a], Norihito Sakaguchi[a], Takahiro Nomura[a], Tomohiro Akiyama[a]*

[a]Center for Advanced Research of Energy and Materials, Hokkaido University, Kita 13 Nishi 8, Kitaku, Sapporo 060-8628, Japan

Abstract

Yellow Ca-α-SiAlON:Eu^{2+} phosphors for white light-emitting diodes (LEDs) were synthesized by a facile combustion synthesis method using CaO, Eu_2O_3, α-Si_3N_4, Si, and Al as raw materials. Ca concentrations and diluent ratios were optimized to improve their luminescence properties. The lattice constant and luminescence properties improved as x increased from 0.4 to 1.2 in $Ca_xSi_{12-(m+n)}Al_{m+n}O_nN_{16-n}:Eu_{0.06}$. The optimum value was x = 1.2. Scanning transmission electron microscopy combined with energy dispersive X-ray analysis detected segregation of Ca and Eu at grain boundaries, which decreased luminescence behavior in the x = 1.4 sample. The influence of Si and Si_3N_4 diluents was investigated by varying the diluent ratio φ = (CaO + Eu_2O_3 + α-Si_3N_4)/(CaO + Eu_2O_3 +α-Si_3N_4 + Al + Si). Changes in temperature and flame propagation speed were measured during combustion synthesis using two thermocouples. When φ was less than 0.5, the combustion temperature exceeded 1600 °C and the synthesized material contained an amount of the high-temperature β-SiAlON phase. At φ > 0.7, the reaction temperature fell below 1200 °C, and unreacted raw materials remained. The optimum value of φ was 0.6. The internal quantum efficiency of the product synthesized at x = 1.2 and φ = 0.6 was approximately 35% under 450-nm excitation. According to electron probe X-ray microanalysis, composition varied within individual synthesized particles, which may explain the decrease in emission behavior relative to a commercial product.

*Corresponding author: Genki Saito

E-mail address: genki@eng.hokudai.ac.jp (G. Saito)

Keywords: phosphor, oxynitride, SiAlON, combustion synthesis

1. Introduction

Rare-earth doped nitride/oxynitride phosphors have attracted much attention for color tuning of white light-emitting diodes (LEDs) owing to their color rendering ability, stability at high temperature, and long lifetime. Eu-doped Ca-α-SiAlON is an alternative to the conventional YAG:Ce phosphor because of its low thermal quenching and high external quantum efficiency [1-4]. Typically, a solid-state reaction [5-9], gas pressure sintering [10, 11], or gas reduction nitridation [12-14] has been used to synthesize Ca-α-SiAlON:Eu^{2+}. However, these methods involve the use of expensive, high-purity α-Si_3N_4 and AlN as starting materials and require prolonged high-temperature sintering (1600–2000 °C) under high nitrogen pressure (1–10 MPa), which is an energy- and time-consuming process. To resolve this problem, combustion synthesis (self-propagation high-temperature synthesis) has been applied to the preparation of Ca-α-SiAlON:Eu^{2+}. Combustion synthesis relies on a strongly exothermic reaction, in which a self-sustaining process occurs. In the case of Ca-α-SiAlON, Si, Al, and CaO are used as raw materials. Because the nitridation of Si and Al is exothermic, combustion occurs continuously within a few tens of seconds of ignition, and external heating after ignition is not necessary. Previous studies of Ca-α-SiAlON:Eu^{2+} combustion synthesis have clarified the effects of NaCl [15, 16], NH_4Cl [17] and initial composition [18]. These reports have demonstrated the efficiency of this method of Ca-α-SiAlON:Eu^{2+} synthesis. However, the emission properties of combustion-synthesized phosphors are low compared to materials prepared by gas pressure sintering, and post-annealing treatment is required [18].

In this study, we examine the effects of Ca concentration and diluent ratios on luminescence properties of phosphors using a heat-insulated porous alumina crucible. To control heat during combustion synthesis, the Si_3N_4 to Si ratio is varied, and the combustion temperature and flame propagation speed are measured using two

thermocouples. The materials obtained are characterized by X-ray diffractometry (XRD) and photoluminescence (PL) measurements. The internal quantum efficiencies of combustion-synthesized and commercial products are determined quantitatively. In addition, cross-sectional elemental analysis of particles is performed using electron probe X-ray microanalysis (EPMA). From these quantitative evaluations, we identify problems and propose strategies for further improvement of combustion synthesis.

2. Material and methods

$Ca_xSi_{12-(m+n)}Al_{m+n}O_nN_{16-n}:Eu_y$ ($m = 2x + 2y$, $m = 2n$, $y = 0.06$) was prepared by varying the Ca content x from 0.4 to 1.4. The m and n are the numbers of Al-N and Al-O bonds substituting Si-N bond, respectively. Because m and n are mutually independent variables, Ca-α-SiAlON with various compositions, including m = 1.5 and n = 1.2[19], m = 1 and n = 1.8[20], m = 2 and n = 1[20], m = 2 and n = 0[21] have been synthesized. In this study, we used the $m = 2n$ as a compositional designing. The raw materials included Si (>99.9%, 5 μm), Al (99.9%, 3 μm), CaO (99.9%), Eu_2O_3 (99.9%), and α-Si_3N_4 (99.9%, 0.5 μm). When Si is used as a raw material, the combustion temperature increases beyond 1800 °C and β-SiAlON tends to stabilize. Therefore, a mixture of Si with Si_3N_4 as diluent was used as a Si source. The weight-based diluent ratio, φ, is defined by the following equation.

$$\varphi = (CaO + Eu_2O_3 + \alpha\text{-}Si_3N_4) / (CaO + Eu_2O_3 + \alpha\text{-}Si_3N_4 + Al + Si) \quad (1)$$

When the effect of Ca content was investigated, the diluent ratio was fixed at 0.6. Subsequently, φ was varied from 0.4 to 0.8 with $x = 1.2$.

A 55-g quantity of starting materials was weighed and mixed for 10 minutes using a mortar and pestle. Figure 1 shows a schematic diagram of the alumina crucible used for combustion synthesis. α-Si_3N_4 powder was added between the crucible and raw material for thermal insulation. A 50-g mixture was loaded into the crucible and softly pressed. A mixture of Al and AlN powder was used as the igniter. Two thermocouples covered by an alumina tube were inserted into the sample. The reactor was evacuated to a pressure below 20 Pa, and nitrogen gas was introduced. The combustion reaction was conducted under nitrogen (99.99%) at 0.8 MPa by passing a 30-A current through a 3-mm wide carbon foil.

The product phases were analyzed by X-ray diffraction (XRD, Miniflex600, Rigaku) using Cu K_α radiation (λ = 1.54056 nm) and a 0.02 ° sampling step. Structural refinements were performed by applying the Rietveld method to powder XRD patterns with the PDXL program (Rigaku) [22, 23]. PL properties were measured using a fluorescence spectrometer (FP-6400, JASCO) at room temperature. Scanning transmission electron microscopy (STEM) combined with energy dispersive X-ray analysis (EDX) was performed using a FEI Titan Cubed G2 60-300 at 300 kV. To distinguish individual elements, a high-angle annular dark-field (HAADF) technique was used, in which the image contrast is roughly proportional to the square of the atomic number, Z [24-26]. For STEM observation, the sample was thinned by cutting, grinding, and ion-milling using a Gatan precision ion-polishing system. The internal quantum efficiencies of combustion-synthesized and commercial products were quantitatively determined using an integrating sphere-equipped (ISF+834, JASCO) fluorescence spectrometer (FP-8500, JASCO) with an excitation wavelength of 450 nm. For cross-sectional elemental analysis of samples, the particles obtained were mixed with fine copper powder and hot-pressed for 1 h at 250 °C to form a bulk

sample, which was cut, polished, and ion-milled using a cross-section polisher (IB-09010CP, JEOL). The elemental composition of 40 samples was determined with a field emission electron probe micro analyzer (JXA-8530F, JEOL). Ca-α-SiAlON:Eu^{2+} phosphor reagent (Sialon Corp.) was used for comparison of luminescence properties.

3. Results and Discussion

3.1 Effect of Ca concentration

When only pure Al and Si are used as raw materials, the combustion temperature becomes extremely high, which causes particle sintering. In our previous work, NaCl was used as a diluent because the heat released from the nitridation of Al is reduced by the NaCl (solid) → NaCl (liquid) reaction (ΔH = 82.1 kJ/mol) [15, 16, 27]. Use of NaCl can decrease particle size by suppressing sintering. However, the presence of Na^+ and Cl^- ions can affect luminescence properties. Therefore, we used α-Si_3N_4 as a diluent without NaCl. The diluent ratio (φ, Eq. 1) was fixed at 0.6 during studies of the effect of Ca concentration. The combustion reaction was successful at Ca contents (x) ranging from 0.4 to 1.4, with the Eu content (y) fixed at 0.06. The XRD patterns of powders synthesized at different Ca contents are shown in Fig. 2. As-prepared powders consisted primarily of a single α-SiAlON crystalline phase at all Ca concentrations, and no β-SiAlON phase was detectable. The right side of Fig. 2 shows an enlargement of the XRD peaks. The shifts in XRD peaks indicate that the α-SiAlON lattice expands with increasing Ca content. The value of m in $Ca_xSi_{12-(m+n)}Al_{m+n}O_nN_{16-n}:Eu_y$ increases as the Ca content increases, and the proportions of Al and O in the material become accordingly larger. Because the Al–O (1.75 Å) and Al–N (1.87 Å) bond distances are larger than that of Si–N (1.74 Å) [11], the crystal lattice expands. According to the Rietveld analysis shown in Fig. 3, the lattice constant of the samples increases with increasing x. This trend is consistent with a previous report [28].

The excitation and emission spectra of Ca-α-SiAlON:Eu^{2+} phosphors prepared with different Ca contents are shown in Fig. 4. The samples exhibit a wide excitation band in the blue region around 380 nm that corresponds to the $4f^7 \rightarrow 4f^65d$ absorption

transition of Eu^{2+} [20, 29, 30]. The emission spectra show a single broad peak at 450–650 nm, which corresponds to the allowed $4f^6 5d \rightarrow 4f^7$ transition of Eu^{2+}. When Eu^{3+} is present, a sharp peak between 560 and 630 nm is observed [30]. This result suggests that the Eu doped into the α-SiAlON host exists as the Eu^{2+} ion. During combustion with Al, the Eu^{3+} in Eu_2O_3 is apparently reduced to Eu^{2+} and then doped into the Ca-α-SiAlON host. The emission intensity of the phosphors increases with increasing Ca content from x = 0.4 to 1.2 as shown in Fig. 4(b). This trend agrees with previous results for Ca-α-SiAlON:Eu^{2+} phosphors [11, 31]. Although the mechanism is as yet unclear, possible reasons for the increase in intensity include: (1) a change in crystal field due to the increased population of O^{2-} ions, and (2) a change in the distribution of Eu atoms in accordance with the lattice expansion. When the Ca content reaches 1.4, the emission intensity decreases significantly. The HAADF-STEM image and STEM-EDS mappings of O, Eu, and Ca are shown in Fig. 5. In Fig. 5(a), the contrast at the grain boundaries is high compared to that of the surrounding grains. From EDS, heavy elements such as Ca and Eu are segregated along the grain boundaries as an oxide-rich phase. The segregated material may be CaO, which comprises a large fraction of the heavy elements in Ca-α-SiAlON:Eu^{2+}. Formation of this segregated oxide decreases the luminescence properties. Segregation was not observed at x = 1.2 and 0.6. In our compositional design based on $Ca_xSi_{12-(m+n)}Al_{m+n}O_nN_{16-n}:Eu_y$, m = 2.92 when x = 1.4 and y = 0.06. Ca-α-SiAlON materials with m > 3 have been synthesized by gas pressure sintering [11]. However, segregation of Ca and Eu occurs in our combustion synthesis. The reaction time of combustion synthesis is relatively short compared to that of gas pressure sintering. Thus, elemental diffusion is not extensive and undoped Ca and Eu remain along the grain boundaries. Based on these results, the optimum Ca content for increasing emission intensity by combustion synthesis is x = 1.2.

3.2 Effect of diluent ratio

Thermal management during combustion synthesis is important for improving emission properties. Based on the results in section 3.1, we investigated the effect of diluent ratio. When φ was varied from 0.4 to 0.8, the combustion reaction was fully complete except for φ = 0.8. At φ = 0.8, too much α-Si_3N_4 diluent decreased the combustion temperature and suppressed continuation of the reaction. Fig. 6(a) shows the temperature histories measured at thermocouples Tc1 and Tc2 with x = 1.2, y = 0.06, and φ = 0.6. After ignition, the temperature increased immediately to a maximum value, and then gradually decreased. The maximum temperature and flame propagation speed are plotted in Fig. 6(b). The temperature decreased with increasing diluent ratio, because the relative amount of Si decreased. Because the thermocouples were covered by an alumina tube, it is possible that the momentary temperature exceeded the measured value. The flame propagation speed was derived from the difference in time required for each thermocouple to achieve its maximum temperature. When the diluent ratio was increased from 0.4 to 0.7, the flame propagation speed decreased from 2.5 to 1.4 mm/s. The decrease in propagation speed is attributed to (1) a decrease in reaction temperature and (2) a decrease in thermal conductivity of the packed raw materials, wherein the diluent was 0.5-μm Si_3N_4 and the reactant was 5-μm Si. Table 1 contains a summary of the temperature measurements during combustion synthesis at different diluent ratios. The holding time to keep the temperature above 1000 °C was increased to ~200–300 sec, because of the increased thermal insulation of the crucible.

Fig. 7(a) shows cross-sectional photographs of materials synthesized with different diluent ratios. When ϕ is less than 0.50, sintered grayish agglomerates are generated at the particle centers. From XRD analysis, these sintered particles contain β-SiAlON and Si. The high-temperature β-SiAlON phase is stabilized because the temperature, especially at the product center, increases as the diluent ratio decreases. When the combustion temperature exceeds the melting point of Si (1414 °C), the Si particles melt and agglomerate. Coarse particle generation prevents the nitriding reaction, which results in unreacted Si. In contrast, the crushability increases at greater diluent ratios. Fig. 7(b) shows the phase ratios determined from XRD patterns with Rietveld refinement. When the diluent ratio is greater than 0.75, the fractions of AlN and α-Si_3N_4 in the synthesized powders increase owing to the decrease in reaction temperature. Thus, the product of greatest purity (>94 mass%) is obtained at $\phi \cong$ 0.55–0.6. The relationship between ϕ and emission intensity at 562 nm under 400-nm irradiation is shown in Fig. 7(c), where the intensity maximum at $\phi = 0.6$ is consistent with this conclusion.

From the above results, a Ca content of $x = 1.2$ and a diluent ratio of $\varphi = 0.6$ represent optimal conditions for the combustion synthesis of Ca-α-SiAlON:Eu^{2+} phosphors. The internal quantum efficiency (IQE) was measured at 450 nm to compare the luminescence properties to those of the commercial product, as shown in Table 2. The IQE of combustion-synthesized phosphors was 35% compared to 73% for the commercial product. The low crystallinity of samples synthesized in the short reaction time of combustion synthesis may be the reason for diminished performance. In addition, elemental non-uniformity may degrade luminescence behavior. To address the role of elemental uniformity, cross-sectioned particle samples were prepared using mechanical and Ar ion milling. The composition of 40 particles was

analyzed quantitatively by field-emission (FE)-EPMA, in which the uniformity of the particles is reflected in the standard deviation of each measurement. 1−3 μm areas at the center of each particle were analyzed with the surface and agglomerates excluded from the measurements. The Eu concentration was 1.19 ± 0.05 wt% in the commercial product and 3.24 ± 1.39 wt% in the combustion-synthesized phosphor. The standard deviations of the Ca, Al, and Si contents also were greater for the combustion-synthesized phosphor, which suggests compositional inhomogeneity. This property apparently is due to the short reaction time and use of a mixture of powders in combustion synthesis. Therefore, further improvements including utilization of flux, increased reaction temperature, post-annealing treatment, and more uniform raw materials will be required.

4. Conclusions

Yellow $Ca_xSi_{12-(m+n)}Al_{m+n}O_nN_{16-n}:Eu_{0.06}$ (x = 0.4–1.4) phosphors were prepared using CaO, Eu_2O_3, Si, Si_3N_4, and Al as raw materials. Ca concentrations and diluent ratios were optimized to improve photoluminescence properties. The lattice constant and luminescence properties increased as x increased from 0.4 to 1.2. The optimum emission intensity occurred at x = 1.2. The diluent ratio φ strongly influenced the reaction temperature. At $\varphi < 0.5$, the combustion temperature exceeded 1600 °C, and the synthesized material contained an amount of the high-temperature β-SiAlON phase. At $\varphi > 0.7$, the reaction temperature was less than 1200 °C and unreacted raw materials remained. The optimum value of φ was 0.6. The internal quantum efficiency of the product synthesized at the optimum condition of x = 1.2 and φ = 0.6 was approximately 35%. Variable composition within individual particles, as determined

by EPMA analysis, may be responsible for the decrease in emission properties. Although combustion synthesis is an energy-efficient method, further improvements will be needed to synthesize uniform materials.

Acknowledgment

We would like to thank the "Nanotechnology Platform" Program of the Ministry of Education for allowing us to conduct STEM observations and EPMA analysis on SiAlON and especially Mr. Kenji Ohkubo, Mr. T. Endo, Mr. Ryo Ota, Mr. T. Tanioka, Ms. Y. Yamanouchi, and Ms. E. Obari for their great technical assistance and helpful suggestions. We also thank Mr. K. Harada (Combustion Synthesis Co., Ltd.). This work was supported by JSPS KAKENHI Grant Number JP17K14805.

References

[1] R.-J. Xie, M. Mitomo, K. Uheda, F.-F. Xu, Y. Akimune, Preparation and Luminescence Spectra of Calcium- and Rare-Earth (R = Eu, Tb, and Pr)-Codoped α-SiAlON Ceramics, Journal of the American Ceramic Society, 85 (2002) 1229-1234.

[2] Y. Fukuda, K. Ishida, I. Mitsuishi, S. Nunoue, Luminescence Properties of Eu2+-Doped Green-Emitting Sr-Sialon Phosphor and Its Application to White Light-Emitting Diodes, Applied Physics Express, 2 (2009).

[3] R.-J. Xie, N. Hirosaki, M. Mitomo, T. Suehiro, X. Xu, H. Tanaka, Photoluminescence of Rare-Earth-Doped Ca-α-SiAlON Phosphors: Composition and Concentration Dependence, Journal of the American Ceramic Society, 88 (2005) 2883-2888.

[4] Z.J. Zhang, O.M. ten Kate, A. Delsing, E. van der Kolk, P.H.L. Notten, P. Dorenbos, J.T. Zhao, H.T. Hintzen, Photoluminescence properties and energy level locations of RE3+ (RE = Pr, Sm, Tb, Tb/Ce) in CaAlSiN3 phosphors, J Mater Chem, 22 (2012) 9813-9820.

[5] Y.Q. Zhang, X.J. Liu, Z.R. Huang, J. Chen, Y. Yang, Photoluminescence properties of Eu2+-Mn2+ codoped Ca-alpha-SiAlON phosphors, Journal of Luminescence, 132 (2012) 2561-2565.

[6] J.J. Yang, Z. Song, L. Bian, Q.L. Liu, An investigation of crystal chemistry and luminescence properties of Eu-doped pure-nitride alpha-sialon fabricated by the alloy-nitridation method, Journal of Luminescence, 132 (2012) 2390-2397.

[7] W.J. Park, Y.H. Song, J.W. Moon, S.M. Kang, D.H. Yoon, Synthesis and luminescent properties of Eu2+ doped nitrogen-rich Ca-α-SiAlON phosphor for white light-emitting diodes, Solid State Sciences, 12 (2010) 1853-1856.

[8] K. Shioi, Y. Michiue, N. Hirosaki, R.-J. Xie, T. Takeda, Y. Matsushita, M. Tanaka, Y.Q. Li, Synthesis and photoluminescence of a novel Sr-SiAlON:Eu2+ blue-green phosphor (Sr14Si68−sAl6+sOsN106−s:Eu2+ (s ≈ 7)), Journal of Alloys and Compounds, 509 (2011) 332-337.

[9] X.W. Zhu, Y. Masubuchi, T. Motohashi, S. Kikkawa, T. Takeda, Synthesis and photoluminescence of blue-emitting 15R-sialon:Eu2+ phosphors, Journal of Alloys and Compounds, 496 (2010) 407-412.

[10] Q. Wu, Y. Wang, Z. Yang, M. Que, Y. Li, C. Wang, Synthesis and luminescence properties of pure nitride Ca-[small alpha]-sialon with the composition Ca1.4Al2.8Si9.2N16 by gas-pressed sintering, Journal of Materials Chemistry C, 2 (2014) 829-834.

[11] R.-J. Xie, N. Hirosaki, M. Mitomo, Y. Yamamoto, T. Suehiro, K. Sakuma, Optical Properties of Eu2+ in α-SiAlON, The Journal of Physical Chemistry B, 108 (2004) 12027-12031.

[12] H.-L. Li, R.-J. Xie, N. Hirosaki, T. Suehiro, Y. Yajima, Phase Purity and Luminescence Properties of Fine Ca-α-SiAlON : Eu Phosphors Synthesized by Gas Reduction Nitridation Method, Journal of The Electrochemical Society, 155 (2008) J175-J179.
[13] H.-L. Li, N. Hirosaki, R.-J. Xie, T. Suehiro, M. Mitomo, Fine yellow α-SiAlON:Eu phosphors for white LEDs prepared by the gas-reduction–nitridation method, Science and Technology of Advanced Materials, 8 (2007) 601-606.
[14] T. Suehiro, N. Hirosaki, R.-J. Xie, K. Sakuma, M. Mitomo, M. Ibukiyama, S. Yamada, One-step preparation of Ca-alpha-SiAlON:Eu[sup 2+] fine powder phosphors for white light-emitting diodes, Applied Physics Letters, 92 (2008) 191904-191903.
[15] Y. Ge, Y. Chen, Q. Wang, W. Cui, Y. Zou, X. Yuan, K. Chen, Effect of NaCl on the properties of Eu-doped Ca-α-SiAlON phosphors prepared by combustion synthesis, Ceramics International, 42 (2016) 4556-4561.
[16] G. Saito, J. Niu, X. Yi, Y. Kunisada, N. Sakaguchi, T. Akiyama, Salt-assisted combustion synthesis of Ca-α-SiAlON:Eu2+ phosphors, Journal of Alloys and Compounds, 681 (2016) 22-27.
[17] Y.-Y. Ge, Y. Chen, Q. Wang, W. Cui, Y.-F. Zou, Z.-P. Xie, X.-Y. Yuan, K.-X. Chen, Effect of NH4Cl additive on combustion synthesis of Eu-doped Ca-α-SiAlON phosphors, Journal of Alloys and Compounds, 654 (2016) 404-409.
[18] Y. Chen, X. Yuan, K. Chen, W. Cui, Y. Ge, Effect of starting composition and post-anneal on the structure and luminescence properties of Eu-doped Ca-α-SiAlON phosphors prepared by combustion synthesis, Journal of Rare Earths, 32 (2014) 501-507.
[19] X. Xu, J. Tang, T. Nishimura, L. Hao, Synthesis of Ca-α-SiAlON phosphors by a mechanochemical activation route, Acta Materialia, 59 (2011) 1570-1576.
[20] J.H. Ryu, Y.-G. Park, H.S. Won, S.H. Kim, H. Suzuki, J.M. Lee, C. Yoon, M. Nazarov, D.Y. Noh, B. Tsukerblat, Luminescent Properties of Ca- alpha -SiAlON:Eu[sup 2+] Phosphors Synthesized by Gas-Pressured Sintering, Journal of The Electrochemical Society, 155 (2008) J99-J104.
[21] H. Zhang, T. Horikawa, H. Hanzawa, A. Hamaguchi, K.-i. Machida, Photoluminescence Properties of alpha-SiAlON:Eu[sup 2+] Prepared by Carbothermal Reduction and Nitridation Method, Journal of The Electrochemical Society, 154 (2007) J59-J61.
[22] H. Rietveld, A profile refinement method for nuclear and magnetic structures, Journal of Applied Crystallography, 2 (1969) 65-71.
[23] F. Izumi, A Software Package for the Rietveld Analysis of X-ray and Neutron Diffraction Patterns, Nihon Kessho Gakkaishi, 27 (1985) 23-31.
[24] R. Huang, Y.H. Ikuhara, T. Mizoguchi, S.D. Findlay, A. Kuwabara, C.A.J. Fisher, H. Moriwake, H. Oki, T. Hirayama, Y. Ikuhara, Oxygen-Vacancy Ordering at Surfaces of Lithium Manganese(III,IV) Oxide Spinel Nanoparticles, Angewandte Chemie International Edition, 50 (2011) 3053-3057.

[25] G. Saito, F. Yamaki, Y. Kunisada, N. Sakaguchi, T. Akiyama, Three-dimensional analysis of Eu dopant atoms in Ca-α-SiAlON via through-focus HAADF-STEM imaging, Ultramicroscopy, 175 (2017) 97-104.
[26] N. Sakaguchi, F. Yamaki, G. Saito, Y. Kunisada, Estimating the dopant distribution in Ca-doped α-SiAlON: statistical HAADF-STEM analysis and large-scale atomic modeling, Microscopy, (2016).
[27] J. Niu, G. Saito, T. Akiyama, A New Route to Synthesize β-SiAlON:Eu 2+ Phosphors for White Light-Emitting Diodes, Applied Physics Express, 6 (2013) 042105.
[28] C.-C. Chung, J.-H. Jean, Synthesis of Ca-α-SiAlON:Eux phosphor powder by carbothermal-reduction–nitridation process, Materials Chemistry and Physics, 123 (2010) 13-15.
[29] K. Sakuma, N. Hirosaki, R.-J. Xie, Red-shift of emission wavelength caused by reabsorption mechanism of europium activated Ca--SiAlON ceramic phosphors, Journal of Luminescence, 126 (2007) 843-852.
[30] K. Shioi, N. Hirosaki, R.-J. Xie, T. Takeda, Y. Li, Photoluminescence and thermal stability of yellow-emitting Sr-α-SiAlON:Eu²⁺ phosphor, Journal of Materials Science, 45 (2010) 3198-3203.
[31] Y. Song, T. Masaki, K. Senthil, D. Yoon, Photoluminescence properties and synthesis of Eu2+-activated Ca-alpha-SiAlON phosphor for white LED application, JOURNAL OF CERAMIC PROCESSING RESEARCH, 14 (2013) S15-S17.

Figure captions

Fig. 1. Schematic diagram of the alumina crucible for combustion synthesis. α-Si_3N_4 powder was added between the crucible and raw material for thermal insulation. The Al/AlN igniter mixture was located at the side of the raw materials, and a carbon foil was inserted into the igniter. Two thermocouples covered by an alumina tube were inserted into the sample.

Fig. 2. XRD patterns of powders synthesized at different Ca contents (x) at a fixed Eu content of y = 0.06 and diluent ratio of ϕ = 0.6. The peaks are consistent with the α-SiAlON structure. The enlarged XRD patterns reveal that the lattice constant increases with increasing x.

Fig. 3. The relationship between Ca content, x, and the lattice constant of samples synthesized at a fixed diluent ratio of ϕ = 0.6.

Fig. 4. (a) Photoluminescence excitation (monitored at 562 nm) and emission spectra (monitored at 400 nm) of samples with different x values. (b) The relationship between x and emission intensity.

Fig. 5. (a) HAADF image of a sample with x = 1.4, in which the bright areas indicate the presence of relatively heavy elements such as Ca or Eu. (b-d) Corresponding STEM-EDX mappings of O, Eu, and Ca.

Fig. 6. (a) Temperature histories measured at W-Re thermocouples Tc1 and Tc2 with alumina tube protection. (b) Maximum temperature and flame propagation speed as a function of the diluent ratio. The maximum temperature is the average value of the two thermocouples. The flame propagation speed is calculated from the difference in time required to reach maximum temperature at the two thermocouples.

Fig. 7. (a) Cross-sectional photographs of materials synthesized with different diluent ratios, (b) phase ratios determined from XRD patterns with Rietveld refinement showing the separation between yellow surface particles and grayish sintered internal material at ϕ <0.50, and (c) relationship between ϕ and normalized emission intensity at 562 nm under 400-nm irradiation.

Table captions

Table 1. Summary of temperature measurements during combustion synthesis at different diluent ratios.

Table 2. The internal quantum efficiency (IQE) measured at 450 nm and results of elemental analysis. Cross-sectioned particle samples for elemental analysis were prepared using mechanical and Ar ion milling. The composition of 40 particles was analyzed quantitatively by FE-EPMA, in which the standard deviation reflects the uniformity of the particles.

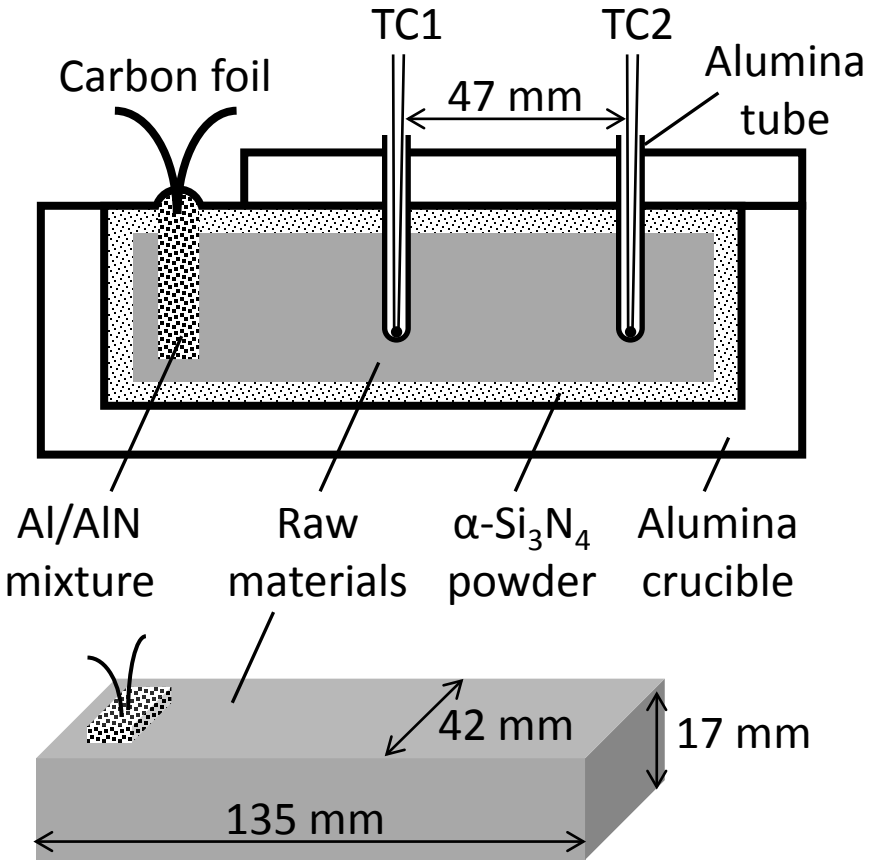

Fig. 1. Schematic diagram of the alumina crucible for combustion synthesis. α-Si_3N_4 powder was added between the crucible and raw material for thermal insulation. The Al/AlN igniter mixture was located at the side of the raw materials, and a carbon foil was inserted into the igniter. Two thermocouples covered by an alumina tube were inserted into the sample.

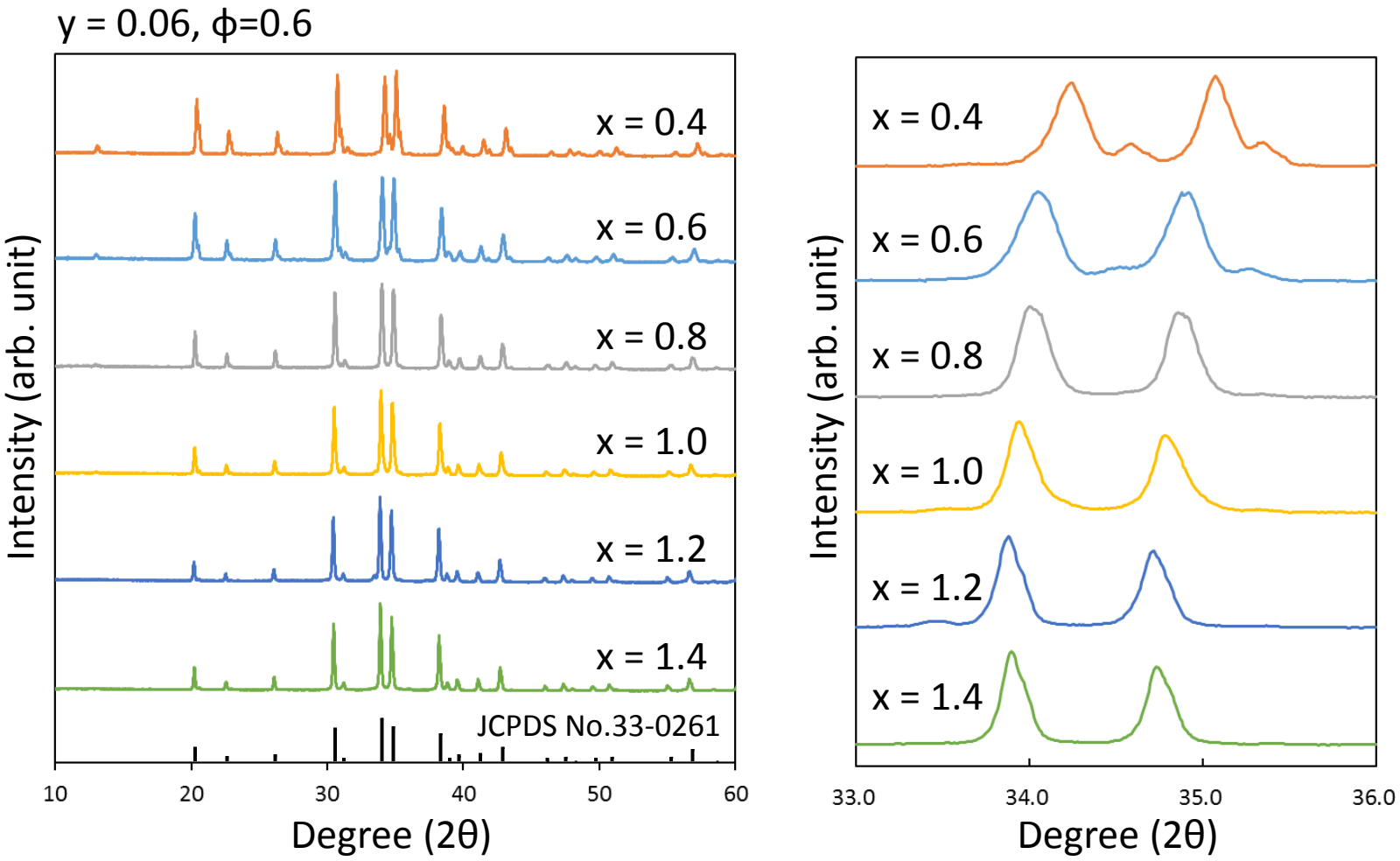

Fig. 2. XRD patterns of powders synthesized at different Ca contents (*x*) at a fixed Eu content of *y* = 0.06 and diluent ratio of ϕ = 0.6. The peaks are consistent with the α-SiAlON structure. The enlarged XRD patterns reveal that the lattice constant increases with increasing *x*.

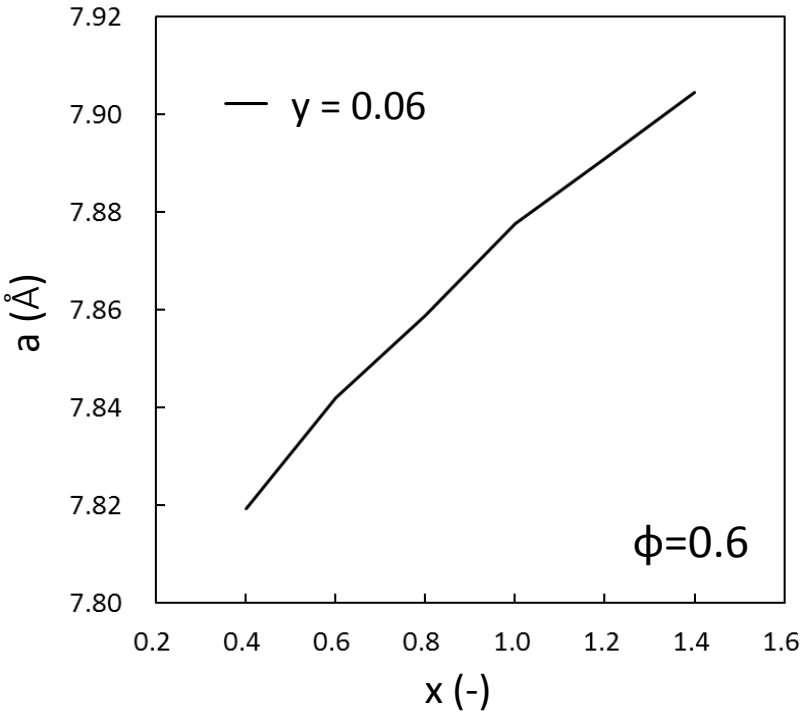

Fig. 3. The relationship between Ca content, *x*, and the lattice constant of samples synthesized at a fixed diluent ratio of ϕ = 0.6.

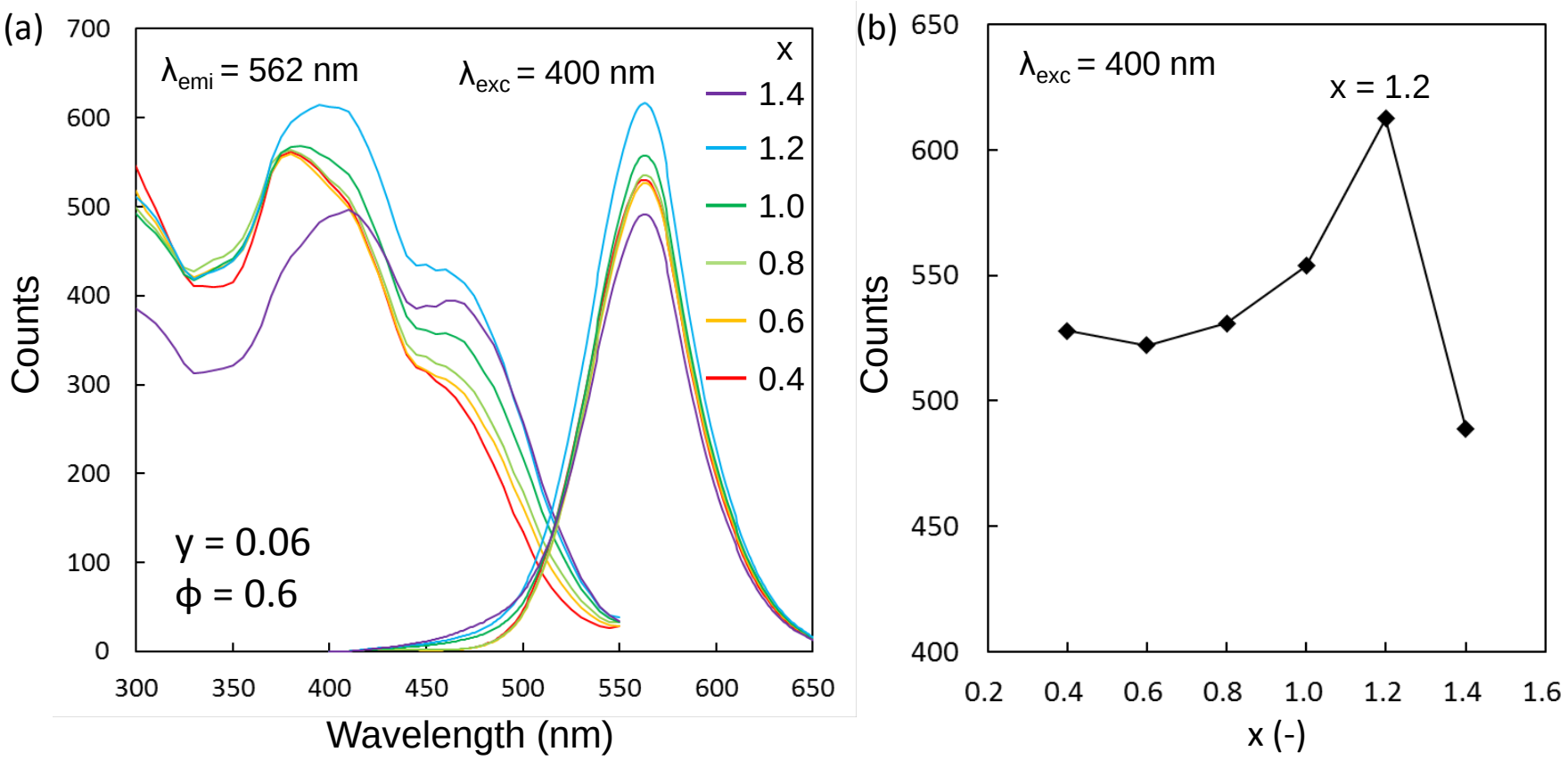

Fig. 4. (a) Photoluminescence excitation (monitored at 562 nm) and emission spectra (monitored at 400 nm) of samples with different *x* values. (b) The relationship between *x* and emission intensity.

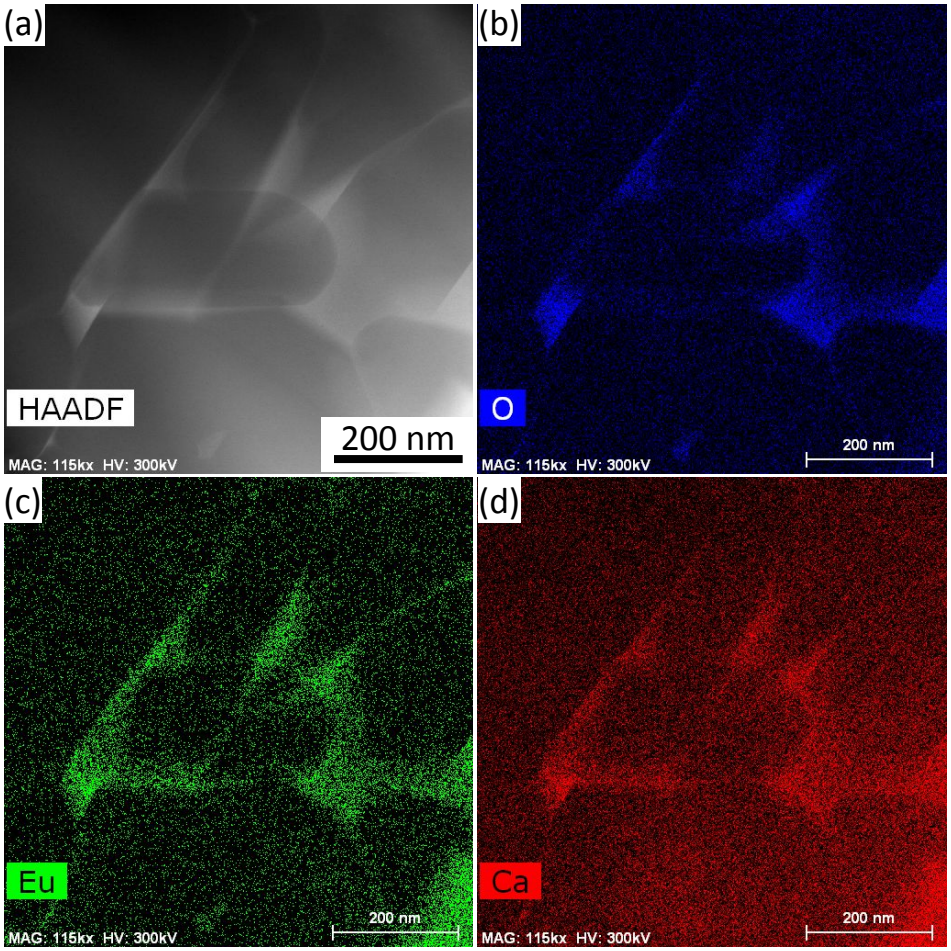

Fig. 5. (a) HAADF image of a sample with x = 1.4, in which the bright areas indicate the presence of relatively heavy elements such as Ca or Eu. (b-d) Corresponding STEM-EDX mappings of O, Eu, and Ca.

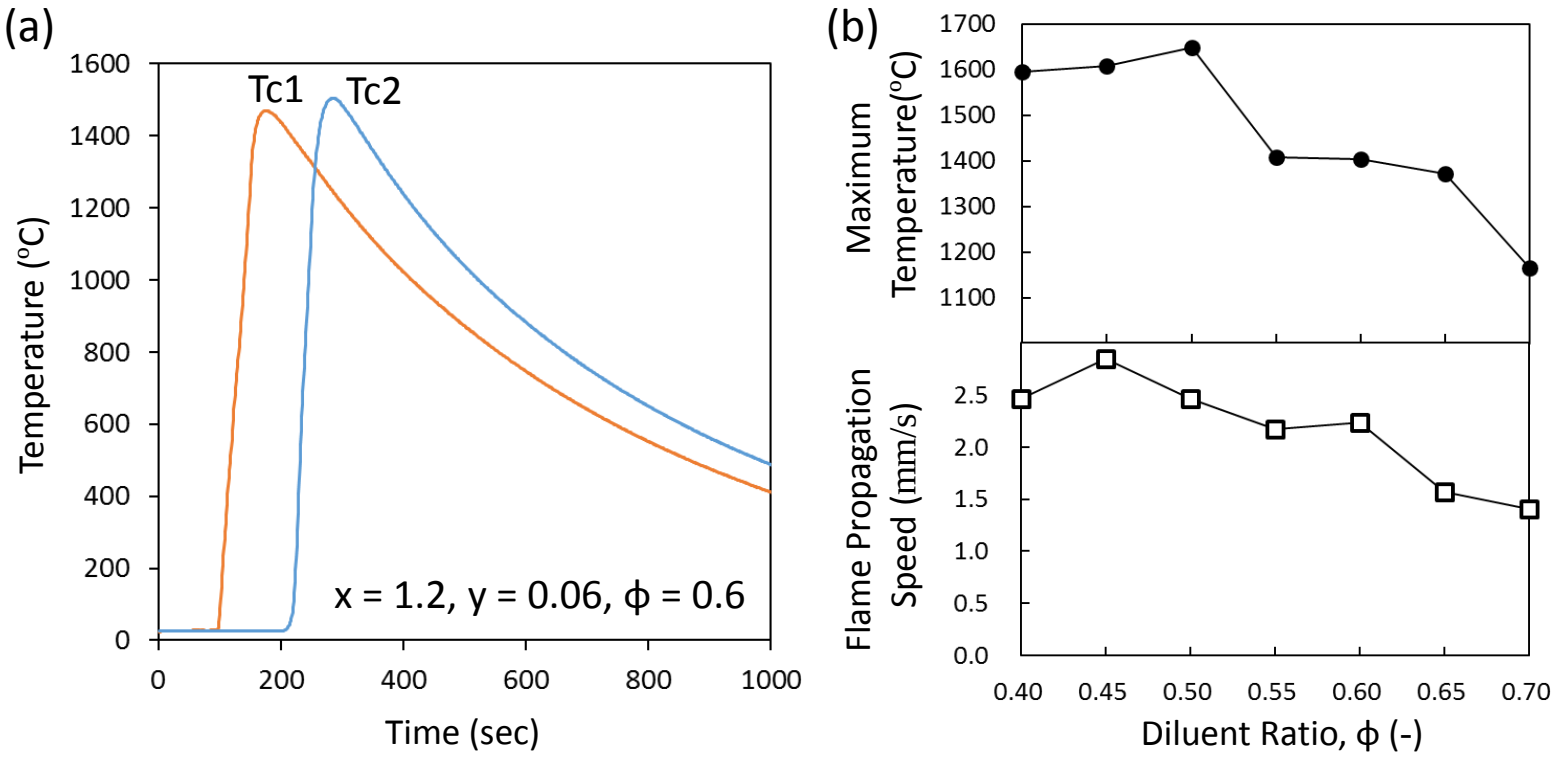

Fig. 6. (a) Temperature histories measured at W-Re thermocouples Tc1 and Tc2 with alumina tube protection. (b) Maximum temperature and flame propagation speed as a function of the diluent ratio. The maximum temperature is the average value of the two thermocouples. The flame propagation speed is calculated from the difference in time required to reach maximum temperature at the two thermocouples.

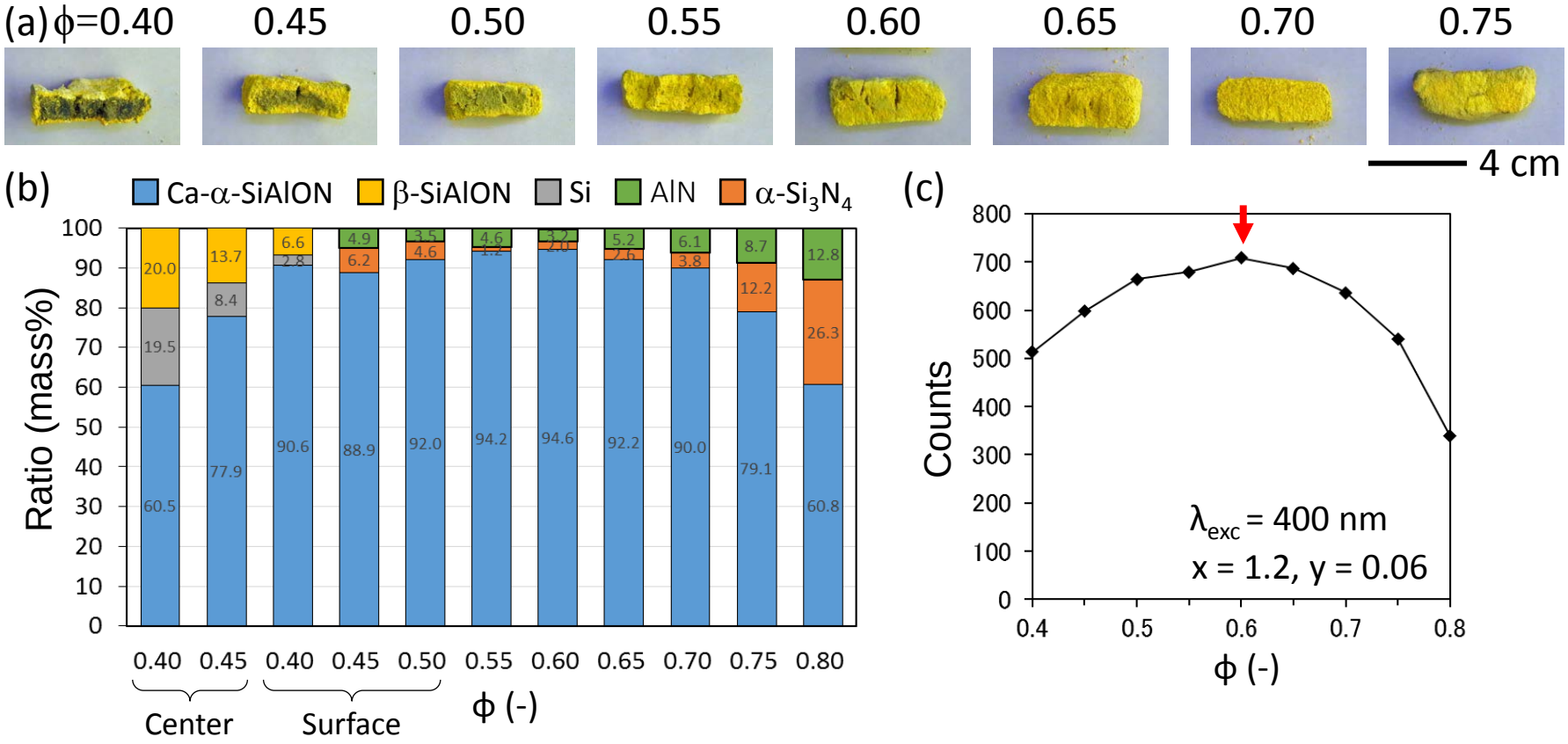

Fig. 7. (a) Cross-sectional photographs of materials synthesized with different diluent ratios, (b) phase ratios determined from XRD patterns with Rietveld refinement showing the separation between yellow surface particles and grayish sintered internal material at ϕ <0.50, and (c) relationship between ϕ and normalized emission intensity at 562 nm under 400-nm irradiation.